Al-Mukhtar Journal of Engineering Research 08 (1): 51-64, 2024
Doi: https://doi.org/10.54172/95e7n966

Research Article

Open Access

The effect of Curing time and temperature on Cathodic Disbondment Behavior of Epoxy-Coated Steel in Marine Environments

Rafaa M. R. Esmaael *, Dawod H. Elabar [2], Mohamed A. Gebril [3], Farag Haidar [4]

***Corresponding author:** rafaa.esmaael@omu.edu.ly, Department of Material Science and Engineering, Faculty of Engineering, Omar Al-Mukhtar University, Libya

[2] Environmental and biological chemistry research center (EBCRC), Tocra, University of Benghazi, Libya

[3, 4] Department of Mechanical Engineering, Faculty of Engineering, University of Benghazi, Libya

Received:
09 September 2024

Accepted:
05 December 2024

Publish online:
31 December 2024

Abstract

Protecting steel structures from corrosion in various environments typically involves coating and cathodic protection. Multiple factors affect the rate at which a coating disbonds, including curing time, temperature, surface preparation, and coating thickness. Numerous research studies have investigated the mechanisms behind blister formation and growth. This study focuses on how the curing temperature affects the number of blisters, blister diameters, and disbanded steel coated with a 100µm epoxy resin. The results show that as the curing time increases for cathodically protected and unprotected samples, the time taken for initial disbonding is prolonged. It is worth noting that the blistering time is longer in polarized samples than in non-polarized ones, regardless of the curing temperature. In addition, blister formation is less frequent in polarized samples than non-polarised ones. As the curing temperature increases, the disbonding area decreases in protected and cathodically unprotected conditions. It has been observed that the size of blisters decreases with higher curing temperatures in protected samples. At the same time, it increases with rising cure temperatures when the system is in protection mode. Notably, the disbonding rates in unprotected samples exceed those in protected samples at all curing temperatures.

Keywords: Epoxy Resin, Coating Disbonding, Sacrificial Anode, Cure Temperature, Marine Environment, Cathodic Protection.

INTRODUCTION

The primary purpose of applying anticorrosive coatings to metallic surfaces, such as steel, is to slow down or impede the natural occurrence of corrosion when exposed to corrosive environments. These coatings comprise several crucial elements, including binders, pigments, fillers, additives, and carriers. They are created using a combination of chemicals and materials in various formulations. Additives can be included in small amounts to improve specific coating properties or address technical problems (Cheng, Fu, Dou, Chen, & Liu, 2023). The carrier acts as a vehicle for the uncured paint constituents but does not play a critical role in the protective mechanisms of the coatings. Besides breaking down the components, the carrier lowers the viscosity of the coating, making it easier to spray or dip. The carrier can be an organic solvent, water, or gas, depending on the type of coating. In liquid form, the carrier is mainly responsible for ensuring adequate coating wetness, thereby controlling film uniformity. Insufficient wetting can result in unprotected areas and film holes (Njoku, Cui, Xiao, Shang, & Li, 2017; Thierry, 2020; Zhang et al., 2018).

The binder provides physical support and containment for pigments and additives, binding these components to the metal surface. Besides providing structure, the binder is crucial for a coating's fundamental properties, such as adhesion to metal, internal cohesion, high mechanical strength, and low permeability. (Knudsen & Forsgren, 2017) .Selecting the correct binder is crucial, as its properties depend on its chemical composition and curing process. The advantages and disadvantages of the chosen binder family play a significant role in coating performance. (Ma, Ammar, Kumar, Ramesh, & Ramesh, 2022) Three pigments are used in anticorrosive coatings: barrier, sacrificial, and inhibitive. They differ in their protective mechanisms and the quantities used in the coating. Sacrificial coatings, such as zinc-rich coatings, need a significant amount of pigment to establish electrical conductivity between the particle and the substrate for protection. Inhibitive pigments rely on the formation of soluble salts at the substrate/paint interface, so they must be present in adequate quantities to facilitate dissolution mechanisms.

Pigments in barrier coatings are chemically inert and act as a barrier against corrosion. (Agwa, Iyalla, & Abu, 2017; Ashassi-Sorkhabi, Moradi-Haghighi, Zarrini, & Javaherdashti, 2012). The quantity and type of pigments significantly influence the mode of protection offered by the coatings, highlighting the importance of selecting the appropriate pigment type and quantity based on the desired protective mechanisms and coating performance. (Kumar & Bhattacharya, 2020; Ramezanzadeh, Bahlakeh, Ramezanzadeh, & Rostami, 2019) Organic coatings are one of the most widely utilized corrosion reduction techniques, and they stand as a prevalent method for inhibiting corrosion in various environments. Adhesion to the substrate is a crucial factor that significantly influences the efficiency of organic coatings as corrosion inhibitors. It is a critical aspect affecting the performance of the coating. (Yu et al., 2021) In recent years, significant efforts have been directed towards enhancing the interaction between surfaces and composite material matrices. Various strategies have been explored for surface modifications aimed at improving interfacial adhesion.

Several methods to achieve the desired result include coatings, in-situ synthesis, and chemical grafting. Several researchers have suggested that hydroxyl ions formed beneath the disbonded coating are responsible for disrupting the bond between the coating and the substrate. (Eyckens et al., 2020; Leng, Streckel, & Stratmann, 1998; Qian & Cheng, 2018). Furthermore, it has been proposed that the diffusion of alkali metal cations accelerates disbonding by supplying them to the disbonding front through the aqueous phase at the interface of the polymer coating. (Rozenfel'd, Rubinshtein, & Zhygalova, 1987; Zhu & Van Ooij, 2002) The initial phase of the cathodic disbonding process is believed to involve water permeation, with the pathway for water movement speculated to occur through channels, capillaries, or pores within the coating. These structural irregularities may arise from the inhomogeneity of curing, impurity particles, or the solubilization of constituents in the coating. (Sato, 1981)

Paint films are not entirely barriers against corrosion agents such as water, oxygen, and ions. They are not impervious to these agents (Hammond, Holubka, DeVries, & Dickie, 1981; Shi et al., 2021) In some cases, the coating film allows too much water and oxygen to pass through, even more than what is typically observed in unpainted metals' corrosion rates. This excessive permeation indicates that factors other than water and oxygen penetration may also contribute to the corrosion rate. If the films of a metal-paint system have low ion diffusion characteristics, it could cause the accumulation of ions at the metal-paint interface due to corrosion reactions. In this case, the formation of hydroxyl ions can result in localized blistering and adhesion issues. This is because the ions struggle to diffuse out easily. Although the corrosion rate may not

be determined by water penetration, it can result in loss of adhesion in a wet state, which could be the deciding factor. Some researchers have suggested that there is a link between the start time and the infiltration of water into the interface. They propose that this infiltration must happen before the disbonding occurs (Chen, Li, Du, & Cheng, 2009; Gaylarde, Morton, Loh, & Shirakawa, 2011; H Leidheiser & Funke, 1987; Leidheiser Jr, Wang, & Igetoft, 1983; Schwenk, 1981; Tsay, 1988)

When steel is polarised cathodically in aerated water, it triggers reactions of oxygen reduction or hydrogen evolution. Two reactions increase pH near the electrode surface.(Babić & Metikoš-Huković, 1993; Esquivel, Olivares, Gayosso, & Trejo, 2011; Jovancicevic & Bockris, 1986) Studies show that the pH in blisters can reach 14. It has been suggested that the disbonding process is associated with a highly alkaline solution (high pH) that exists between the coating and the metal substrate (Koehler, 1984; Henry Leidheiser, 1981) Degradation and potential failure can occur during service due to several factors. There are several reasons why coatings on steel substrates can fail. These may include insufficient surface preparation, inadequate coating application, mechanical damage from backfilling, and stress, among other possible factors. (LeBozec, Thierry, & Pelissier, 2018).

This study aims to investigate how the curing time of epoxy resin, when used on a steel substrate and combined with cathodic protection in seawater, impacts the disbonding process. The presence or absence of a connection to an aluminum alloy sacrificial anode is also considered. Specifically, a 6 mm defect deliberately created in the coating facilitates ingressing water, oxygen, and reactive ions to the metal substrate. This condition leads to easier cathodic disbonding, which varies among samples due to differences in curing temperatures and whether the sample was subjected to polarization. The investigation examines the impact of curing temperatures and polarization while keeping coating thickness, potential, bath temperature, coating type, and substrate nature constant across all samples. The results show a clear correlation between initiation time and curing temperature.

MATERIALS AND METHODS

Working electrode

In electrochemical experiments, the working electrode is where redox reactions occur. Cold-rolled mild steel plates measuring 0.8mm in thickness, 15mm in length, and 7.5mm in width were used for this experimental investigation. This study chose mild steel plates based on their frequent use as the primary construction material in marine environments.

Reference electrode

The reference electrode is an essential component in electrochemical experiments. It stabilizes and produces a known electrical potential against which the working electrode's potential is measured. The study utilized a standard laboratory-type saturated calomel electrode (SCE) as a reference electrode to ensure accurate and reproducible electrochemical measurements. The Standard Calomel Electrode (SCE) is a widely used reference electrode in electrochemical measurements owing to its stability and precise potential value. It plays a crucial role in maintaining a consistent electrical potential, against which the working electrode's potential can be accurately measured in various electrochemical analyses and experiments.

Sacrificial anode

A sacrificial anode is a metal component intentionally placed within a system or structure to protect other important metal surfaces from corrosion. It functions as a sacrificial element by

readily corroding instead of the metal it is meant to protect. This effectively prevents corrosion on the protected surface and prolongs the life of the metal structure. Usually made of a metal or alloy that naturally corrodes, the sacrificial anode is connected electrically to the metal it protects. When an object is submerged in an electrolyte like seawater or soil, the sacrificial anode corrodes preferentially, releasing electrons that flow to the protected metal, effectively suppressing its corrosion. In this work, aluminum sacrificial anodes were used. The table below shows the anode composition provided by Trident Alloys Ltd for Imp Alloy III, an Al-Zn-In alloy.

Table (1). Composition of anode alloy

Element	Zn	In	Fe	Si	Cu	Ga	Ti	Al
Composition wt.%	4.5	0.0175	0.083	0.086	0.0024	0.0082	0.0198	Remainder

Paint

During the experiments, epoxy resin paint from H. MARCEL GUEST Ltd have been used. To apply the paint, the base lacquer mixed with the hardening or curing agent in a 3:1 weight ratio, following the supplier's recommended instructions for preparation and application. The applied paint consisted of a chlorinated rubber "high build-up protective coating" and a mixture of beeswax and colophony resin in a ratio of 3:1. The experiment's electrolyte was a 3% sodium chloride solution.

Equipment

For the experiments, the potential difference was measured using a high-resistance digital voltmeter. The electrochemical cell was made by using a 15-liter plastic tank, which is shown in Figure 1. To measure the thickness of the dry paint, an Elcometer 256FN instrument was used.

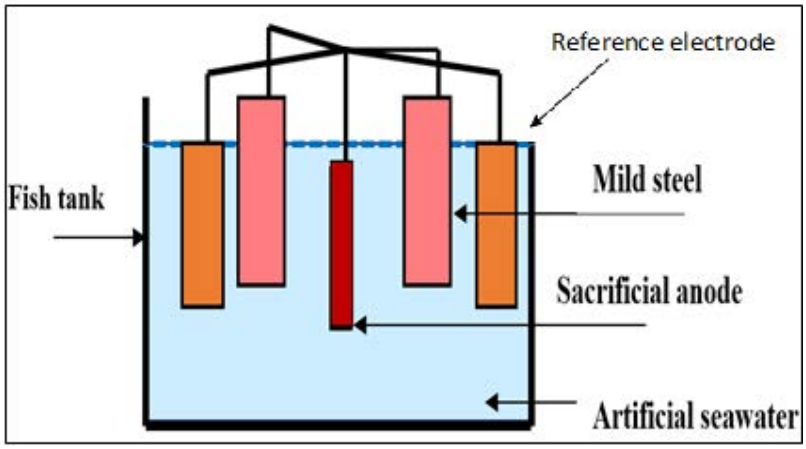

Figure.(1). The electrochemical cell

Sample preparation

The process involved a necessary degreasing step to eliminate all traces of grease from the plates. This was achieved by wiping all the plates multiple times with ethanol and drying them using a stream of hot air until completely dry.

Coating procedures

After blending the lacquer and hardener in a 3:1 ratio, entrapped air bubbles were eliminated by gently mixing the mixture and leaving it undisturbed for 10 to 15 minutes before application. In

order to achieve a smooth and even surface for application, a waiting period was necessary. To attach the plate to the steel plate and achieve the desired wet film thickness, two pieces of cellophane tape were overlapped on both sides of the panel. A small quantity of paint was poured onto the top edge of the plates. Then, a drawbar spreads the paint evenly, ensuring a consistent and reproducible coating thickness. The painted plates were left to cure at room temperature for one hour. Four samples underwent two different conditions:

1. Four samples were left at room temperature for three days.
2. four samples were subjected to 50°C in an oven for three days.
3- Four samples underwent different heating conditions: two sets were placed in an oven at 80°C and 100°C for two days, and another set was placed in an oven at 100°C for three days.
4- Three samples were placed in an oven at 100°C for four days.

The impact of different curing temperatures and durations on painted plates was examined under varying conditions.

Thickness measurement

The dry paint thickness for each sample was measured at various points across the coated panels, and the average was calculated to fall within the range of 100µm. The Elcometer model number 256FN was used to measure paint thickness accurately.

Final Sample Preparation

An intentional defect was created in the coated samples by drilling a 6mm diameter hole in the paint. Three coats of chlorinated rubber were applied to protect the edges and rear of the painted plates, with drying time allowed between each coat. A layer of beeswax mixed with colophony resin was applied over the chlorinated rubber, protecting only the painted area from the bath environment. "To investigate the effect of curing temperature on the disbonding rate, all aspects related to the material and preparation of specimens, including the type and thickness of the coating, the sodium chloride bath, the sacrificial anode, and other variables, were kept consistent across all test sets." The only variables that changed were the curing temperature and whether the samples were polarized through the aluminum sacrificial anode or were left unpolarized.

Cathodic Polarization

The schematic diagram in Fig.1 shows the experimental setup. The samples were connected to the sacrificial anode. In contrast, one sample from each curing condition was left unconnected to the sacrificial anode, which is left in an "open circuit" condition. The painted samples were subjected to an electrochemical cell setup using an aluminum alloy sacrificial anode to induce cathodic polarization. This polarization occurred at approximately -1.1 volts concerning the saturated calomel electrode (SCE) while maintaining room temperature.

Cathodic Disbonding Measurement

After a certain period, the samples that had been coated were removed from the bath and rinsed with distilled water. Then, they were gently wiped with tissue paper. Transparency sheets were placed over the samples to trace the disbonded areas accurately. Systematic measurements and tracing of disbanding areas were conducted to monitor their progression over time.

RESULTS AND DISCUSSION

Table 2 shows the time it takes for blisters to form at different curing temperatures. The samples were tested with and without connection to a sacrificial anode.

Table (2). Effect of curing temperature on the blistering initiation time

Blister initiation time (hours)	Curing temperature		
	Room temperature	50 °C	100 °C
T_o hours "polarized samples"	108	240	288
T_o hours "not polarized samples"	48	98	144*

T_o is blistering initiation time per hours
* for this cure temperature, no blister appeared during the experiment, but the artificial defect diameter gradually increased.

Table (2) shows that curing temperature significantly affects blister initiation time for polarized and nonpolarized systems. The data indicates that blister initiation time increases with higher curing temperatures. It was observed that the samples that were not polarized started to disbond earlier than the polarized samples. This shows that polarization effectively delayed the disbonding process, making it clear that it had a protective influence in this experimental setup. The change in blister number with time (dn/dt) as a function of curing temperatures is presented in Table (3). It shows a distinct pattern in the number of blisters observed in polarized samples.

Table (3). Change in blister number as a function of curing temperatures

Change in blister Number	Curing temperature		
	Room temperature	50 °C	100 °C
dn/dt "polarized samples"	0.09	0.08	0.015
dn/dt "not polarized samples"	0.104	0.11	---*

dn/dt is the change in blister number as a function of immersion time
*No blisters appeared, and the diameter of the defect increased gradually.

As the curing temperature increases, the number of blisters decreases. On the other hand, in the open circuit system, the number of blisters remains relatively consistent between samples cured at room temperature and those cured at 50 °C. Interestingly, there were no blisters observed in samples that were cured at 100 °C in the open circuit system during this experiment. This difference in blister formation between the two curing temperatures suggests that temperature varies depending on blister formation, especially when no polarization is present. In this specific experiment for the open circuit system, it was observed that no blisters appeared in samples cured at 100 °C. This discrepancy in the blister formation between curing temperatures may suggest that temperature has varying effects on blister formation, especially when there is no polarization. For all samples and different cured temperatures, the number of blisters increased with immersion time, regardless of whether the samples were polarized with the sacrificial anode or at the open circuit with the sacrificial anode, as shown in Fig. 2. The observed trends in blister initiation for the polarized and open circuit systems, at varying curing temperatures, reveal unexpected findings.

In the polarized system, samples cured at room temperature initiated more disbonding than those cured at 50 °C and 100 °C, with the latter exhibiting the least initial blistering. This trend contradicts the assumption that samples cured at higher temperatures should have fewer initial blisters, as the unprotected system shows. Samples cured at 50 °C in the open circuit showed a higher number of initial blisters as compared to those cured at room temperature. This finding contradicts the conventional expectation that samples cured at room temperature should have more initial blisters than those cured at 50 °C. These unexpected observations may indicate intricate interactions among curing temperature, polarization, and the blister initiation process. Other factors in this experimental setup that are not yet fully understood could have an influence as well. Samples that were polarized and cured at room temperature started to disbond with more initial blisters than those cured in an open circuit at the same temperature. However,

samples cured at 50 °C in a polarized system started to disbond with the same number of initial blisters as those cured in an open circuit system. Blisters increased more in an open circuit system than in the polarized system at all curing temperatures over time.

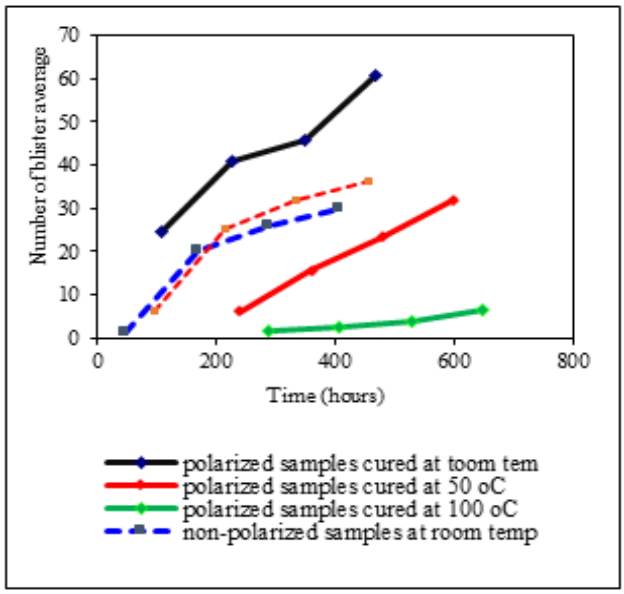

Figure (2). Average number of blisters as a function of time

Fig. 3 shows a significant impact of curing temperature on initial disbonding areas observed in the samples. Disbonding started after 108 hours in the polarized samples cured at room temperature, with an initial disbonding area of approximately 67 mm². Samples cured at 50 °C showed disbanding initiation after 240 hours, with a disbonding area of 39 mm², whereas those cured at 100 °C displayed disbanding after 288 hours with an approximate disbonding area of 7 mm². In the samples where the sacrificial anode was used, disbonding started after 48 hours, and the initial disbonding area was three mm². For the samples cured at 50 °C, disbonding started after 96 hours, and the disbonding area was 64 mm². However, disbanding was not observed in the samples cured at 100 °C during the experimental duration.

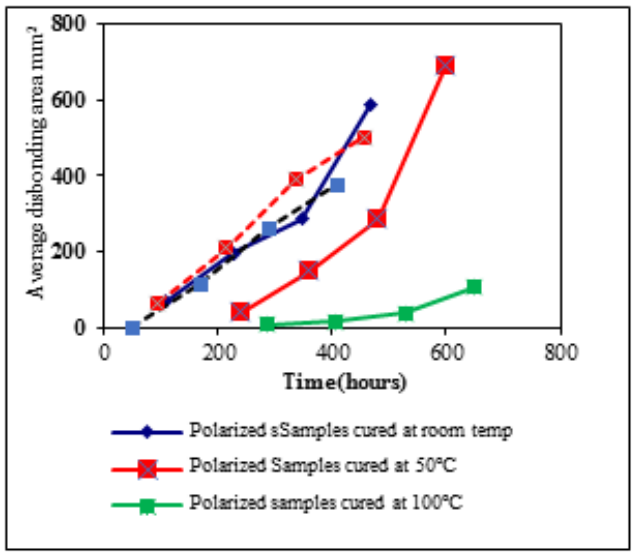

Figure (3). Average desponding area as a function of time

The results highlight the significant effect of the curing temperature on the initiation and extent of disbonding. These findings indicate a consistent pattern where higher curing temperatures lead to delayed disbonding initiation and reduced initial disbonding areas in both open circuit and polarized systems.

Fig.3 shows that samples cured at room temperature disbonded earlier than polarized samples despite exhibiting similar disbonding rates initially. After around 350 hours, there was a noticeable rise in disbonding rate for the polarized samples. However, the disbonding rate for the open-circuit samples remained pretty consistent. Additionally, the open circuit samples cured at 50 °C started to disband earlier and with a larger initial area than the polarized samples. Initially, both systems had a similar disbonding rate. However, after 480 hours, the polarized samples showed a significant increase in disbonding rate, diverging from the consistent rate observed in the open circuit samples.

The polarized and open circuit samples showed divergent disbonding behavior over time despite their initial similarities in disbonding rates. This shift became particularly evident during extended durations, showcasing a distinct change in disbonding rates between the two systems. The pivotal moment was the significant increase observed in the disbonding rate of the polarized samples. The disbonding rate in closed-circuit samples showed a significant increase, in contrast to the relatively consistent and sustained disbonding rate observed in open-circuit samples. This difference highlights the dynamic nature of disbonding behavior and how factors like polarization status and other variables can influence it. It also emphasizes that the evolution of disbonding rates over time can be significantly influenced by these factors in this experimental context. The information presented in Table 4 illustrates the effect of curing temperature on disbonding rates (dA/dt).

The samples were cured over three days. The results indicate that polarized samples cured at 100°C exhibited a lower disbonding rate than those cured at 50°C and ambient temperature. However, there was only a marginal difference in disbonding rates between samples cured at 50°C and those cured at ambient temperature. This experiment demonstrates that a higher curing temperature of 100°C significantly reduces the disbonding rate in polarized samples. This highlights the importance of curing conditions on disbonding behavior in this experimental setup.

Table (4). Change in disbonding rate with relation to curing temperature

Curing temperature	Room temperature	50°C	100°C
(dA/dt) mm^2/hrs “polarized samples”	1.63	1.44	0.33
(dA/dt) mm^2/hrs “not polarized samples”	2	1.54	---*

*The change in the artificial defect diameter was tiny

The table data indicates that curing temperature significantly impacts the disbonding rate in open circuit samples. A clear trend exists where the disbonding rate decreases with increasing curing temperature. Higher curing temperatures are linked to lower disbonding rates in open-circuit samples. Furthermore, comparing open circuit and polarized samples reveals interesting findings. In particular, when the samples were cured at room temperature, it was observed that the rate of disbonding in the open circuit samples was significantly higher than that in the polarized samples. However, when the samples were cured at 50°C, the data did not show a significant difference in the disbonding rates between the open circuit and polarized samples. This highlights the intricate relationship among curing temperature, polarization status, and their im-

pact on disbonding rates, demonstrating varying effects in diverse scenarios. Table 5 shows how the average blister diameter changed over time for all samples under different conditions as a function of curing temperature. Consistent with all samples and conditions tested in the experiment, the observed trend shows that blister diameter increases with time. This implies that blister diameters grow or enlarge consistently and progressively over time, regardless of curing temperature or other studied variables.

Table (5). Blister diameter changes as a function of curing temperature

Curing temperature	Room temperature	50 °C	100 °C
(db/dt) mm/hrs "polarized samples"	$6.15x10^{-3}$	$4.3x10^{-3}$	$5.3x10^{-3}$
(db/dt) mm/hrs "not polarized samples"	$6.06x10^{-3}$	$1.2x10^{-3}$	*

*No blisters appeared; the diameter of the defect increased gradually.

Based on the given information, it seems that Table 5 shows the rate of change in the average size of blisters for polarized samples. This suggests that the rate does not depend on the curing temperature. It appears that Fig. 4 visually represents the initial blister sizes for samples cured at different temperatures. The initial blister diameter is lower at room temperature than at 100°C. Samples cured at 50°C display intermediate diameter.

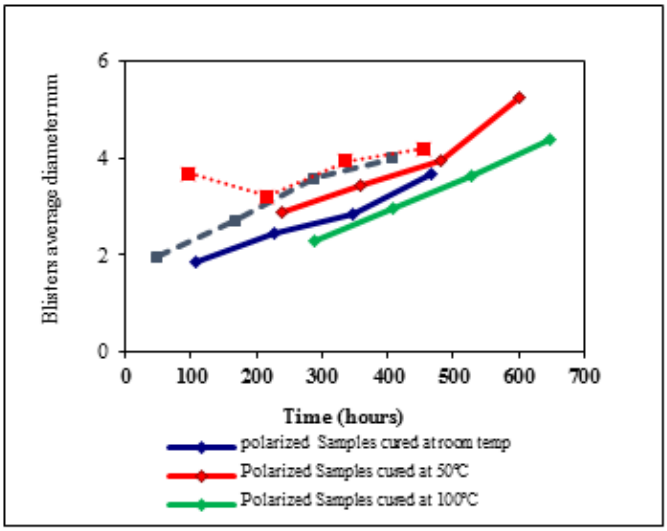

Figure (4). Blisters' average diameter as a function of time

This observation highlights that while the rate of change in blister diameter over time may not be directly associated with curing temperatures in polarized samples, the initial blister diameter does exhibit variation concerning curing temperatures. According to the trend observed, the samples cured at room temperature show the lowest initial blister diameter, followed by those cured at 100 °C, and then by samples cured at 50 °C. This distinction emphasizes the potential impact of curing temperature on the initial development or formation of blisters in the experimental setup. The information provided shows stimulating observations regarding the blister diameter changes in curing temperature and polarization status. Samples cured at room temperature and in an open circuit system exhibit a faster blister diameter increase than samples cured at 50 °C. Fig. 4 shows that samples cured at 50 °C have a larger average blister diameter than those cured at room temperature and in an open circuit.

The size of blisters, the rate of change, and polarization status have intricate relationships with curing temperature. Blister diameter changes and initial diameters vary between samples cured

at different temperatures and under varying polarization, indicating the complexity of factors influencing blister formation and growth. Based on the description in Fig. 4, there are noticeable differences in the initial blister average diameter between polarized samples cured at room temperature and those cured in an open circuit system. The graph displays encouraging patterns in the evolution of blister diameters as time passes. Samples treated with polarized curing at room temperature demonstrate an initial average blister diameter smaller than the samples in an open circuit system. It's important to note that blister diameters behave differently over time. After approximately 288 hours, the average blister diameter stabilizes or reaches a steady state in an open circuit system. However, for polarized samples, the average blister diameter continues to increase beyond 348 hours.

These observations suggest that initial blister sizes differ between polarized samples cured at room temperature and those in an open circuit. However, there are also divergent trends in blister diameter behavior over time. This may suggest that the polarization status and curing temperature influence the initial sizes and the long-term behavior or growth patterns of blisters in the experimental setup. This observation emphasizes that although the rate of change in blister diameter over time might not be directly associated with curing temperatures in polarized samples, the initial blister diameter does showcase variation concerning curing temperatures. The data suggests that the size of initial blisters is smallest in samples cured at room temperature, followed by those cured at 100°C, and then by samples cured at 50°C. This observation indicates that curing temperature may impact the formation of blisters in the experiment. Based on the information provided, there are interesting findings regarding the changes in blister diameter related to curing temperature and polarization status. Samples cured at room temperature and in an open circuit system displayed a faster increase in blister diameter compared to samples cured at 50°C. Fig. 4 shows that samples cured at room temperature and in open circuit initially have a smaller average blister diameter than samples cured at 50°C.

These results indicate complex relationships between curing temperature, polarization status, rate of change, and initial blister sizes. The observed differences in blister diameter changes and initial diameters among samples cured at various temperatures and under different polarization statuses highlight the complexity of factors influencing blister formation and growth in this experimental context. Based on the information provided in the description of Figure 4, there seem to be significant variations in the average diameter of blisters at the beginning between the polarized samples cured at room temperature and the samples in an open circuit system. The figure also depicts encouraging patterns in how these blister diameters change over time. Polarized samples cured at room temperature display a smaller initial average blister diameter compared to samples in open circuit systems. Notably, there is a difference in blister diameter behavior over time. In an open circuit system, the average blister diameter of samples usually reaches a steady state after about 288 hours. On the other hand, for polarized samples, the average blister diameter tends to keep increasing even after 348 hours. Upon curing at room temperature, polarized samples exhibit differences in initial blister sizes and varying trends in blister diameter behavior over time. This suggests that the polarization status and curing temperature affect the initial blister size and their long-term growth patterns in the experiment.

It seems that the samples cured at 50°C exhibit a behavior similar to those cured at room temperature, as shown in Fig. 4, concerning the trends in blister diameter. The key difference is the timing at which particular changes occur in these blister diameters. Blister average diameter behavior in polarized and open circuit systems for samples cured at 50°C follows a trend similar to that observed in room-temperature cured samples. However, there is a difference in the tim-

ing of significant changes. In samples with polarization, the average diameter of blisters tends to increase after being cured for 480 hours at 50°C. However, in samples with an open circuit system cured at the same temperature, the blister diameter reaches a steady state or plateau much earlier, at around 338 hours. This finding suggests that although the blister diameter behavior of samples cured at room temperature and 50°C may appear similar, the timing of crucial changes in blister growth or stabilization varies. This indicates that the curing temperature and polarization status may nuanced the blister evolution over time. After curing at 100°C and polarization, the samples were tested by immersing them in brine water. The results showed that blisters appeared after 288 hours of immersion.

The samples that were cured at room temperature and 50°C had larger blister diameters (compared to those cured at 100°C), and the average blister diameters increased steadily with an increase in immersion time. The most minor blister diameters observed were 2.2 mm^2. The samples that were cured at a temperature of 100°C with an open circuit and a sacrificial anode did not develop any blisters on their surface. In all cases, the initial blisters appeared near the defect and then spread to the rest of the sample. In summary, while mechanical and chemical processes can contribute to blister expansion, the experiment suggests hydrostatic pressure is the predominant driving force. It is believed that the consistent growth rates of blisters, regardless of polarization status, support the inference that regions at the interface have varying degrees of adhesion, ranging from good to poor. Likely, blisters form initially in areas where the adhesion is relatively weaker. This suggests that the degree of adhesion is a key factor in the formation of blisters. As blisters form in certain areas, the water that diffuses from existing blisters will open new blister sites. When the temperature reaches 100 C, the epoxy must be more cross-linked, and the adhesion should be improved. Furthermore, any residual solvent will be evaporated at this temperature. This explains the improvement in performance by reducing oxygen, water, and ion transport due to improved barrier properties.

CONCLUSION

The current work's key conclusions can be presented as follows:

1. The initial blistering time significantly increases with higher curing temperatures in unprotected and protected samples.
2. Polarized samples consistently exhibit longer initial blistering times than non-protected samples at all curing temperatures.
3. Blister development rates increase with curing temperature for protected and non-protected samples.
4. The rate of change in blister number is higher for non-protected samples than protected ones at all curing temperatures. In protected samples, initial blister numbers decrease with higher curing temperatures, while blister numbers increase in nonprotected samples with increased curing temperature.
5. The rate of disbonding increases as the curing temperature rises for protected and unprotected samples. Unprotected samples show higher disbonding rates than protected samples. However, the disbonding rate for protected samples tends to increase to higher rates after a specific time.
6. The rate of blister diameter change is higher in protected samples than in unprotected samples.
7. Average blister diameter decreases with time in unprotected samples but increases in protected samples.

These conclusions demonstrate the intricate relationship among curing temperatures, polariza-

tion, and various factors that affect blistering, disbonding, and changes in blister diameter over time.

Duality of interest: The authors declare that they have no duality of interest associated with this manuscript.

Author contributions: Contribution is equal between authors.

Funding: No specific funding was received for this work.

REFERENCES

Agwa, O., Iyalla, D., & Abu, G. (2017). Inhibition of bio corrosion of steel coupon by sulphate reducing bacteria and Iron oxidizing bacteria using Aloe Vera (Aloe barbadensis) extracts. *Journal of Applied Sciences and Environmental Management, 21*(5), 833-838.

Ashassi-Sorkhabi, H., Moradi-Haghighi, M., Zarrini, G., & Javaherdashti, R. (2012). Corrosion behavior of carbon steel in the presence of two novel iron-oxidizing bacteria isolated from sewage treatment plants. *Biodegradation, 23*, 69-79.

Babić, R., & Metikoš-Huković, M. (1993). Oxygen reduction on stainless steel. *Journal of applied electrochemistry, 23*, 352-357.

Chen, X., Li, X., Du, C., & Cheng, Y. (2009). Effect of cathodic protection on corrosion of pipeline steel under disbonded coating. *Corrosion Science, 51*(9), 2242-2245.

Cheng, X., Fu, M., Dou, W., Chen, S., & Liu, G. (2023). Accelerated degradation of cathodic protected epoxy coating by Pseudomonas aeruginosa in seawater. *Construction and Building Materials, 408*, 133640.

Esquivel, R. G., Olivares, G. Z., Gayosso, M. H., & Trejo, A. G. (2011). Cathodic protection of XL 52 steel under the influence of sulfate reducing bacteria. *Materials and Corrosion, 62*(1), 61-67.

Eyckens, D. J., Demir, B., Randall, J. D., Gengenbach, T. R., Servinis, L., Walsh, T. R., & Henderson, L. C. (2020). Using molecular entanglement as a strategy to enhance carbon fiber-epoxy composite interfaces. *Composites Science and Technology, 196*, 108225.

Gaylarde, C., Morton, L., Loh, K., & Shirakawa, M. (2011). Biodeterioration of external architectural paint films–a review. *International Biodeterioration & Biodegradation, 65*(8), 1189-1198.

Hammond, J., Holubka, J., DeVries, J., & Dickie, R. (1981). The application of x-ray photo-electron spectroscopy to a study of interfacial composition in corrosion-induced paint de-adhesion. *Corrosion Science, 21*(3), 239-253.

Jovancicevic, V., & Bockris, J. M. (1986). The mechanism of oxygen reduction on iron in neutral solutions. *Journal of the Electrochemical Society, 133*(9), 1797.

Knudsen, O. Ø., & Forsgren, A. (2017). *Corrosion control through organic coatings*: CRC press.

Koehler, E. (1984). The mechanism of cathodic disbondment of protective organic coatings—aqueous displacement at elevated pH. *Corrosion, 40*(1), 5-8.

Kumar, V., & Bhattacharya, A. (2020). Demand for Low-VOC Coatings Continues to Rise. *Paint & Coatings Industry*.

LeBozec, N., Thierry, D., & Pelissier, K. (2018). A new accelerated corrosion test for marine paint systems used for ship's topsides and superstructures. *Materials and Corrosion, 69*(4), 447-459.

Leidheiser, H. (1981). Corrosion control by organic coatings.

Leidheiser, H., & Funke, W. (1987). Water disbondment and wet adhesion of organic coatings on metals: A review and interpretation. *Journal of the Oil and Colour Chemists' Association, 70*(5), 121-132.

Leidheiser Jr, H., Wang, W., & Igetoft, L. (1983). The mechanism for the cathodic delamination of organic coatings from a metal surface. *Progress in Organic Coatings, 11*(1), 19-40.

Leng, A., Streckel, H., & Stratmann, M. (1998). The delamination of polymeric coatings from steel. Part 2: First stage of delamination, effect of type and concentration of cations on delamination, chemical analysis of the interface. *Corrosion Science, 41*(3), 579-597.

Ma, I. W., Ammar, S., Kumar, S. S., Ramesh, K., & Ramesh, S. (2022). A concise review on corrosion inhibitors: types, mechanisms and electrochemical evaluation studies. *Journal of Coatings Technology and Research*, 1-28.

Njoku, D. I., Cui, M., Xiao, H., Shang, B., & Li, Y. (2017). Understanding the anticorrosive protective mechanisms of modified epoxy coatings with improved barrier, active and self-healing functionalities: EIS and spectroscopic techniques. *Scientific reports, 7*(1), 15597.

Qian, S., & Cheng, Y. F. (2018). Degradation of fusion bonded epoxy pipeline coatings in the presence of direct current interference. *Progress in Organic Coatings, 120*, 79-87.

Ramezanzadeh, M., Bahlakeh, G., Ramezanzadeh, B., & Rostami, M. (2019). Mild steel surface eco-friendly treatment by Neodymium-based nanofilm for fusion bonded epoxy coating anti-corrosion/adhesion properties enhancement in simulated seawater. *Journal of Industrial and Engineering Chemistry, 72*, 474-490.

Rozenfel'd, I., Rubinshtein, F., & Zhygalova, K. (1987). Corrosion Protection of Metals by Paint Coatings: Khimiya, Moscow.

Sato, Y. (1981). Mechanism and evaluation of protective properties of paints. *Progress in Organic Coatings, 9*(1), 85-104.

Schwenk, W. (1981). Corrosion Control by Organic Coatings. *Adhesion Loss of Organic Coatings—Causes and Consequences for Corrosion Protection*, 103.

Shi, L., Song, G., Li, P., Li, X., Pan, D., Huang, Y., . . . Guo, Z. (2021). Enhancing interfacial performance of epoxy resin composites via in-situ nucleophilic addition polymerization

modification of carbon fibers with hyperbranched polyimidazole. *Composites Science and Technology, 201*, 108522.

Thierry, D. (2020). Powder and High-Solid Coatings as Anticorrosive Solutions for Marine and Offshore Applications? A Review. *Coatings, 10*(10), 916.

Tsay, K. (1988). *The failure of organic coatings during cathodic protection.* University of Manchester.

Yu, M., Fan, C., Ge, F., Lu, Q., Wang, X., & Cui, Z. (2021). Anticorrosion behavior of organic offshore coating systems in UV, salt spray and low temperature alternation simulated Arctic offshore environment. *Materials Today Communications*, *28*, 102545.

Zhang, F., Ju, P., Pan, M., Zhang, D., Huang, Y., Li, G., & Li, X. (2018). Self-healing mechanisms in smart protective coatings: A review. *Corrosion Science*, *144*, 74-88.

Zhu, D., & Van Ooij, W. J. (2002). Structural characterization of bis-[triethoxysilylpropyl] tetrasulfide and bis-[trimethoxysilylpropyl] amine silanes by Fourier-transform infrared spectroscopy and electrochemical impedance spectroscopy. *Journal of adhesion science and technology*, *16*(9), 1235-1260.